

TRANSFER REACTIONS WITH RADIOACTIVE BEAMS NEAR THE $N = 50$ AND $N = 82$ SHELL CLOSURES*

RICCARDO ORLANDI

Advanced Science Research Center, Japan Atomic Energy Agency
Tokai, Ibaraki, 319-1111, Japan

(Received January 26, 2016)

Knowledge of single-particle energies is critically important for a microscopic description of the atomic nucleus. In the absence of a model capable of accurate predictions across the whole nuclear chart, realistic calculations still require that effective single-particle energies be empirically determined. Transfer reactions are one of the best tools to determine the single-particle strength of the populated states, by comparing the experimental and theoretical cross sections of the scattered light ejectiles. Radioactive ion beams and new experimental set-ups are being used to study transfer reactions in inverse kinematics in increasingly exotic regions of the nuclear chart. In this context, studies of nuclei neighbouring single and double shell closures are particularly valuable, because they permit direct comparisons with the latest shell model calculations. This paper will focus, in particular, on measurements carried out near the $N = 50$ and $N = 82$ neutron shell closures, which cross respectively the neutron-rich doubly-magic exotic nuclei ^{78}Ni and ^{132}Sn .

DOI:10.5506/APhysPolB.47.803

1. Introduction

In the endeavour to understand and describe the considerable reorganization which shell structure undergoes away from the valley of stability [1, 2], exotic doubly-magic nuclei provide a unique testing ground for nuclear theory. Doubly-magic nuclei such as ^{78}Ni , ^{100}Sn , ^{132}Sn , or the recently discovered ^{54}Ca [3], and their neighbours, are the key systems to test our theoretical understanding, since the proximity of the doubly-magic core makes shell-model calculation feasible. Furthermore, the study of these systems

* Presented at the XXXIV Mazurian Lakes Conference on Physics, Piaski, Poland, September 6–13, 2015.

provides experimental quantities which are the essential ingredients of the shell model, such as single-particle energies and matrix elements of the effective interaction.

When experimental data are scarce, single-particle and single-hole energies are often assumed to coincide with the energies of low-lying excited states of nuclei neighbouring doubly-magic nuclei, measured, for example, via γ spectroscopy. This method is only acceptable as a working assumption, in the absence of direct-reaction data. Even in the near proximity of magic numbers, in fact, the single-particle strength can be distributed among many different excited states. A recent theoretical work by Coraggio *et al.* [4], on neutron-rich tin and antimony isotopes, highlights how rapidly the strength becomes fragmented among different states. The simple addition of a neutron pair to ^{133}Sb ($Z = 51$, $N = 82$) reduces the single-particle strength of several low-lying states in ^{135}Sb to below 50%. In ^{137}Sb , the full strength is not recovered even by summing the strength of the lowest 15 calculated states. As it will be shown in the following section, the available data does not permit to test these predictions. Hence, as it becomes experimentally feasible, the single-particle strength of excited states neighbouring shell closures ought to be experimentally quantified.

The extent of the single-particle character of a nuclear state can be empirically measured with the aid of single-nucleon transfer reactions. Such reactions studies permit to determine, within certain uncertainties, the spectroscopic factors (SFs) of the populated states, via the comparison between the theoretical and experimental differential cross sections of the scattered light ejectiles. The measurement of the purity of the single-particle character of the populated state is the object of current debates (see, for example, [5–8]). Despite the uncertainties, transfer reactions remain the privileged tool to determine effective single-particle energies and their evolution away from the valley of stability. If the spectroscopic factors are measured for all the states corresponding to transfer to the same orbit, effective single-particle energies can be deduced from the weighted sum of the individual state energies. The aim of this brief contribution, however, is simply to highlight the selectivity and inductive inference of this kind of experiments.

First, a brief review of single-nucleon transfer and single-nucleon pick-up measurements carried out near the $N = 82$ and $N = 50$ shell closures will be given. This summary is limited to experiments using radioactive ion beams. Closer to the stability line, most of the experiments which could be done with stable beams and targets were performed in the 1960s and 1970s. There are, however, some recent and important exceptions that are worth mentioning, such as the extensive systematic measurements of $N = 83$ and $N = 51$ isotones using stable beams and targets, by Kay *et al.* [9] and Sharp *et al.* [10]. In Sections 3 and 4, the specific cases of ^{131}Sn ($Z = 50$,

$N = 81$) and ^{79}Zn ($Z = 30$, $N = 49$) will be presented in more detail. To conclude, few comments will be given about future experimental possibilities and projects to extend transfer studies in these regions.

2. Brief summary of available measurements

Figures 1 and 2 summarize the available transfer data near ^{132}Sn and ^{78}Ni . The corresponding published works are cited in the figure caption. With the sole exception of the study of ^{135}I , no reaction involving proton transfer or removal has been performed, due to experimental challenges such as the detection of neutron ejectiles, in the case of the (d, n) reaction, or gas targets, in the case of the $(^3\text{He}, d)$ or $(^4\text{He}, t)$ reactions. The proton-removal reaction $(d, ^3\text{He})$ is instead limited by the large negative Q -value for reactions with neutron-rich nuclei. For example, in the case of ^{132}Sn , the study of this reaction would require accelerated ^{132}Sn beam energies of the order of 10 MeV/ u . It is also worth pointing out that among the measurements using radioactive ion beams (in grey/light green in the figures), 10 out of 11

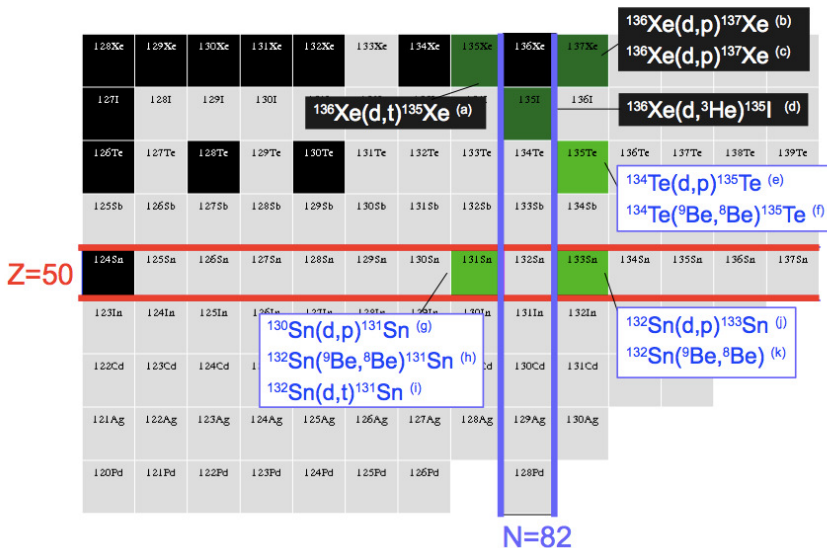


Fig. 1. (Colour on-line) Isotopes studied via single-nucleon transfer reactions along the $N = 82$ shell closure, in the neighbourhood of ^{132}Sn , using stable (dark grey/dark green, direct kinematics) or radioactive (grey/light green, inverse kinematics) ion beams. (a)Schneid and Rosner, 1966 [14]; (b)Moore, 1978 [15]; (c)Kay, 2011, in inverse kinematics [16]; (d)Wildenthal, 1971 [17]; (e)Pain, unpublished; (f)Allmond, 2012 [18]; (g)Kozub, 2010 [19]; (h)Allmond, 2014 [20]; (i)Orlandi, unpublished; (j)Jones, 2010 [21]; (k)Allmond, 2014 [20].

employed the accelerated Holifield Radioactive Ion Beam Facility (HRIBF) beams at Oak Ridge National Laboratory, before the regrettable shutdown. In the region of ^{78}Ni , the doubly-magic shell closure is even harder to access, as revealed by Fig. 2.

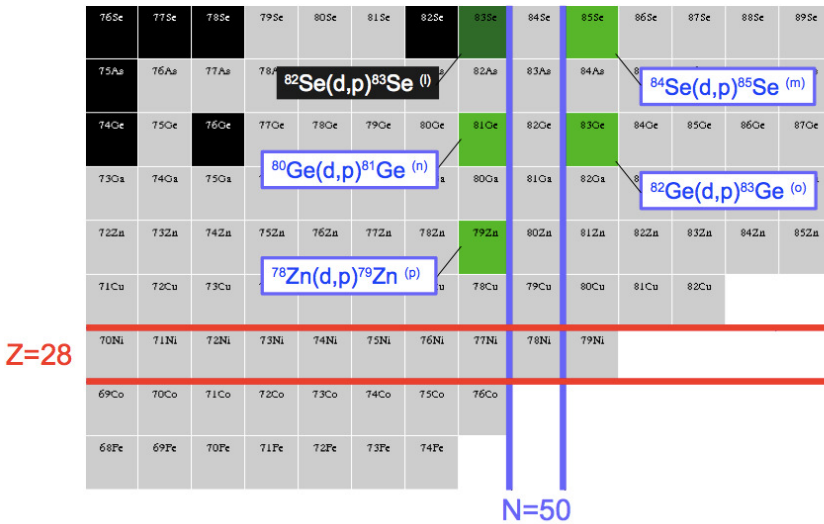


Fig. 2. (Colour on-line) Isotopes studied via single-nucleon transfer reactions along the $N = 50$ shell closure, in the neighbourhood of ^{78}Ni . ^(l)Montestrucque, 1978 [22]; ^(m)Thomas, 2007 [23]; ⁽ⁿ⁾Ahn, 2013 [24]; ^(o)Thomas, 2005 [25]; ^(p)Orlandi, 2015 [28].

3. ^{131}Sn and neutron-hole states below the $N = 82$ shell closure

Even though the first spectroscopic studies of ^{132}Sn date back to the 1970s [11], the nearest neighbours of ^{132}Sn are still mostly known only from β decay [12, 13]. Only during the last few years, ^{132}Sn neighbours were studied via transfer reactions. In particular, the work by Jones *et al.* [21] on single-neutron states in ^{133}Sn populated using a neutron-stripping reaction, was the first transfer measurement with a ^{132}Sn beam. The single-neutron spectroscopic factors measured by Jones turned out to be consistent with shell-model expectations. These states were later observed also via a sub-Coulomb transfer reaction by Allmond *et al.* [20]. ^{131}Sn was also studied via transfer by Kozub *et al.* [19], using the $^{130}\text{Sn}(d,p)$ reaction in inverse kinematics. By adding one neutron to ^{130}Sn , only states *above* the $N = 82$ gap could be populated. These one-particle, two-holes states all lie above 2.5 MeV and match very well the ^{133}Sn states observed by Jones *et al.* [21].

In their work, however, Kozub *et al.* [19] did not populate any of the low-lying ^{131}Sn states shown in Fig. 3. This did not come as a surprise, since they likely correspond to neutron-hole states below the $N = 82$ shell closure. To populate them via transfer, it is necessary to remove a neutron from ^{132}Sn . Until recently, these states were known exclusively from β decay. The only exception is the work by Allmond *et al.* [20], who populated the 331 keV ($1/2^+$) state with the $^{132}\text{Sn}(^9\text{Be},^{10}\text{Be})^{131}\text{Sn}$ sub-Coulomb reaction. From the intensity of the observed 331 keV de-exciting transition, and by comparison with the theoretical total cross section calculated in the DWBA approximation, a SF = 4(3) was deduced for this state. The large uncertainty is mainly introduced by the DWBA modelling of single-neutron pick up using fairly heavy ions like ^9Be , very sensitive to the chosen bound-state parameters.

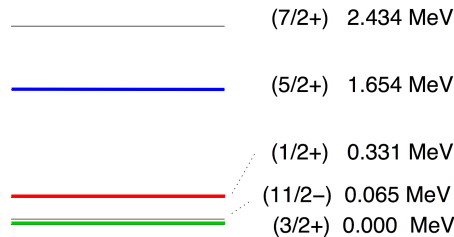


Fig. 3. (Colour on-line) Low-lying states in ^{131}Sn . The states populated in the reaction are highlighted in colour.

In order to quantify more precisely the amount of single-hole strength in these low-lying states, and with the aim of testing the tentative spin-parity assignments, the $^{132}\text{Sn}(d,t)^{131}\text{Sn}$ reaction was performed at HRIBF. In the experiment, the radioactive ^{132}Sn beam was accelerated to ~ 4.39 MeV/ u (579 MeV) by the Oak Ridge TANDEM accelerator, with an intensity of approximately 10^4 pps. The beam impinged on a thin, $250 \mu\text{g}/\text{cm}^2$ deuterated polyethylene target. The tritons ejected in the reaction were detected using the SuperORRUBA array of segmented Si telescopes [29]. The tritons were discriminated from other charged particles (elastic deuterons, transfer protons, *etc.*) by their $\Delta E-E$ energy deposition signature on the PID plot, shown in Fig. 4.

One of the main difficulty in the study of (d,t) reactions in inverse kinematics is that the tritons are emitted only at forward angles. For the beam energy chosen in this experiment, the reaction kinematics yield a double-valued distribution from 0 to approximately 50 degrees in the laboratory angle. At small angles (< 35 degrees), the tritons could not be fully stopped in the Si detectors. Furthermore, low-energy tritons corresponding to the low-energy branch of the distribution could not be identified because they

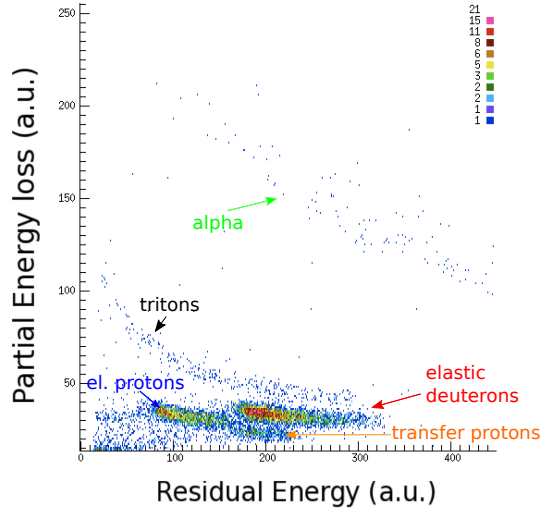


Fig. 4. (Colour on-line) ΔE energy loss *versus* residual energy identification plot.

stopped in the ΔE detectors. Unfortunately, low-energy tritons are those corresponding to the lowest centre-of-mass angle, *i.e.* where the differential cross section yields the most reliable determination of the spectroscopic factor. The effective angular range covered by SuperORRUBA went from approximately 35 to 50 degrees in the laboratory. In the centre-of-mass frame, these angles correspond to a range from 33 to 95 degrees for the ^{131}Sn ground state. A large fraction of the emitted tritons can, however, be expected to be observed within this range, as shown by the zero-range DWBA calculation performed using TWOFNR [26] shown in Fig. 5. The

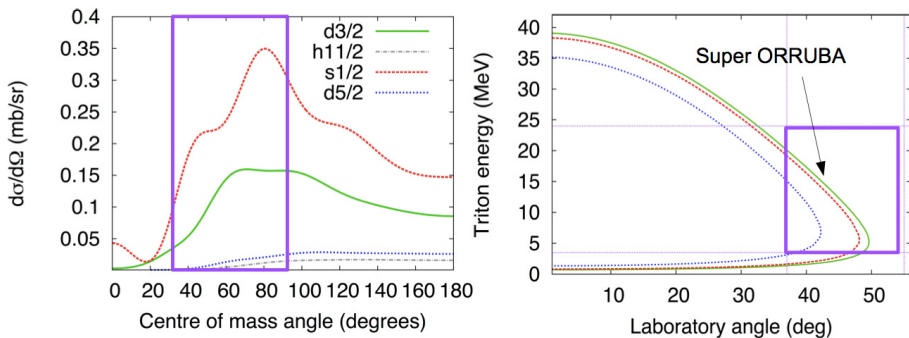


Fig. 5. (Colour on-line) (Left) Calculated angular distributions in the centre-of-mass frame using DWBA calculations, in the zero range approximation. The $d_{3/2}$ and $s_{1/2}$ states have the largest cross sections. (Right) Kinematic lines of tritons ejected in the $^{132}\text{Sn}(d, t)$ reaction, corresponding to population of the lowest d and s states in ^{131}Sn . The grey/purple square defines the range observed by the Si array.

(d, t) reaction kinematics offers, however, two important advantages: the curvature of the distribution provides calibration points for the angular calibration, and the large triton energies reduce the straggling in the target and result in good energy resolution.

The typical response of one of the seven SuperORRUBA telescopes employed in the measurement is shown in Fig. 6, where the detected triton energies are plotted against the laboratory angle. The detected tritons follow very closely the theoretical kinematic lines, permitting to separation between the ground state and the state at 331 keV. More details on the analysis and the results are the object of a forthcoming publication [27].

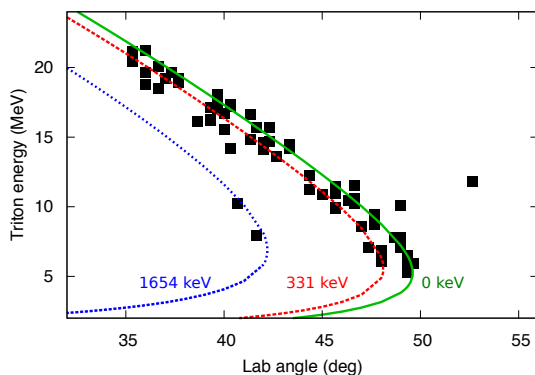


Fig. 6. Kinematic plot of tritons detected in one of the seven SuperORRUBA Si telescopes. The calculated kinematic lines correspond to the population of ^{131}Sn states respectively at 0, 331, and 1654 keV.

4. ^{79}Zn and neutron-single particle states near ^{78}Ni

The other measurement discussed here is the neutron-transfer reaction $^{78}\text{Zn}(d, p)^{79}\text{Zn}$, which was carried out in inverse kinematics at REX-ISOLDE, CERN [28]. The main motivation for this experiment was to achieve the first spectroscopic study of ^{79}Zn ($Z = 30$, $N = 49$), and the measurement of the single-particle strength of the populated states. An additional scope was to shed light on the magicity of ^{78}Ni , and, in particular, on the size of the $N = 50$ shell gap, which has been the object of contrasting predictions, from as low as 3 to 5 MeV. In the chosen reaction, the neutron could be transferred to orbits both below and above the $N = 50$ gap. The ^{79}Zn spectrum, and, in particular, the energy of the single-particle states based on orbits above the gap, such as $\nu d_{5/2}$ and $\nu s_{1/2}$, can be taken as a clear indication of whether the gap size is shrinking or increasing when approaching ^{78}Ni . Moreover, transfer to low- ℓ orbits such as s , p and d was favoured by the chosen beam energy.

In the experiment, a radioactive ^{78}Zn beam accelerated to 2.83 MeV/ u by the REX-ISOLDE Linac impinged on deuterated polyethylene targets. The protons ejected in the reaction were detected using the T-REX segmented Si array [30], and the reaction chamber was surrounded by the Miniball Ge array [31]. Further details on the experimental set-up and the analysis can be found in [28]. The scope of this presentation is, in particular, to highlight the power of the combined detection of transfer ejectiles (in this case protons) and γ rays emitted by ^{79}Zn excited states populated in the reaction. From the analysis of the charged-particle data, the excitation spectrum of ^{79}Zn could be deduced, and it is shown on the left-hand side of Fig. 7. It shows three main peaks, respectively at 1.2, 2.5 and 3.3 MeV. The right-hand side of Fig. 7 shows the Doppler-corrected ^{79}Zn γ -ray spectrum, gated on two different excitation energy regions. For example, if the excitation energy is restricted to the lowest energy peak, only the 441 and 983 keV lines can be seen in the spectrum.

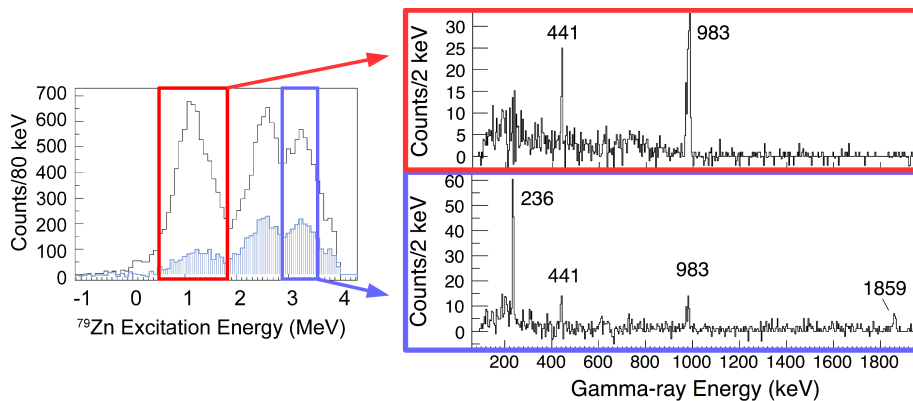


Fig. 7. (Left) ^{79}Zn excitation energy spectrum deduced from proton kinematics. The area highlighted in black/blue is the same spectrum gated on any γ . (Right) ^{79}Zn Doppler-corrected γ -ray spectra gated on different excitation-energy regions. Modified from [28].

The possibility of gating on different excitation energy regions, together with two observed coincident pairs of transitions, proved to be essential to determine the ^{79}Zn level scheme, shown in Fig. 8. In particular, the 236 keV γ ray could not have been placed on the level scheme without the excitation-energy data, since it corresponds to the de-excitation of a state not populated by transfer, but fed from above. The observed coincidence between the 236 and the feeding 1858 keV transitions, combined with the corresponding excitation energy spectrum, led to the identification of a state at 1.35(15) MeV

which decays to a state 236 keV below, *i.e.* at 1.10(15) MeV. Because no coincidence could be seen between the 236 keV and the 983 keV transition, the state at 1.10(15) MeV is a long-lived isomer.

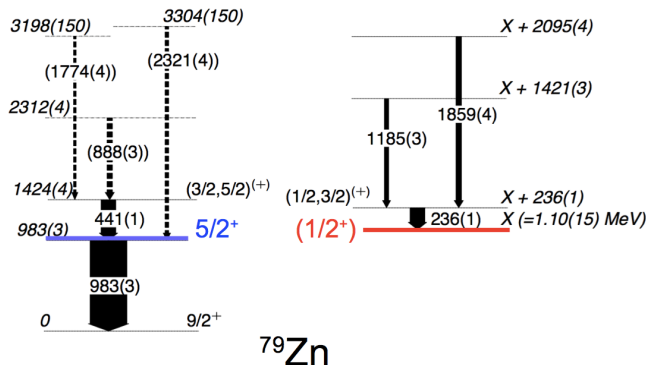


Fig. 8. Level scheme of ^{79}Zn deduced from the combined analysis of proton and γ -ray data. With the exception of the isomeric state ‘X’ at 1.10(15) MeV, all energies are in keV, with the error in brackets. Modified from [28].

The analysis of proton angular distributions gated by γ -ray transitions, discussed in [28], led to a $5/2^+$ assignment for the state at 983 keV. The γ -ungated angular distributions reveal however also a strong amount of $\ell = 0$ transfer ($\text{SF} \sim 0.4$) in the excitation energy range 0.85–1.55 MeV, centered approximately at 1.05 MeV. This $\ell = 0$ component in the angular distribution is not observed when gating on the 983 keV γ ray. The isomeric state at 1.10(15) MeV is therefore most likely a $1/2^+$ state. The large error bar is due to the uncertainty in the excitation energy due to the limited proton resolution, and is compatible with a $1/2^+$ isomer lying either above or below the $5/2^+$ state. In both cases, the isomerism can be explained with electromagnetic selection rules, *i.e.* either a long-lived E2 transition in the μs or ms range, or an E4 transition to the $9/2^+$ ground state, in the ms range. For the state decaying via the 236 keV γ ray, a $1/2^-$ assignment is favoured by the lack of direct population and by systematics. The intense feeding however from higher states cannot exclude a positive parity assignment. The comparison of the energy of the lowest excited states in ^{79}Zn with large-scale shell-model calculations by Sieja and Nowacki [32] support the picture of a robust magicity of ^{78}Ni , with an $N = 50$ gap of approximately 4.7 MeV. More details can be found in [28].

5. Future possibilities

The importance of transfer reactions to understand shell evolution is witnessed by the fact that such kind of experiments are on the priority list of most radioactive-ion-beam facilities. The combination of charged particle and γ -ray detection is also recognized as a powerful tool to study transfer reactions with exotic beams. This is despite the internal limitation due to the opposite requirements on target thickness: as thick as possible to improve the statistics for γ -ray detection, but as thin as possible to optimize the resolution in the charge-particle detection. In addition to the T-REX+Miniball at ISOLDE, one could mention, among others, the GODDESS+Gammasphere at Argonne National Laboratory, SHARC+TIGRESS at TRIUMF, or the future TRACE+GALILEO/AGATA at LNL, Legnaro.

In order to overcome the lack of knowledge on proton single-particle and single-hole strengths, reactions like (t, α) , $(d, {}^3\text{He})$, $({}^7\text{Li}, {}^6\text{He})$ are already feasible and likely to be carried out using such set-ups. It is also worth mentioning the cryogenic gas-cell target which can be installed in the HELIOS solenoid spectrometer [33], which will permit to study proton-transfer reactions such as $({}^4\text{He}, t)$.

This work was partly supported by the Spanish Project MEC Consolider — Ingenio 2010, Project No. CDS2007-00042 (CPAN), the Marie Curie Actions Contract PIEFGA-2011-30096, and in part by the U.S. Department of Energy, Office of Science, Office of Nuclear Physics, and used the Holified Radioactive Ion Beam Facility, a D.O.E. Office of Science User Facility, and the National Science Foundation.

REFERENCES

- [1] R. Kanungo, *Phys. Scr.* **T152**, 014002 (2013).
- [2] T. Otsuka, *Phys. Scr.* **T152**, 014007 (2013).
- [3] D. Steppenbeck *et al.*, *Nature* **502**, 207 (2013).
- [4] L. Coraggio *et al.*, *Phys. Rev. C* **87**, 034309 (2013).
- [5] J.P. Schiffer *et al.*, *Phys. Rev. Lett.* **108**, 022501 (2012).
- [6] R.J. Furnstahl, H.-W. Hammer, *Phys. Lett. B* **531**, 203 (2002).
- [7] K.L. Jones *et al.*, *Phys. Rev. C* **84**, 034601 (2011).
- [8] A.E. Lovell, F.M. Nunes, *J. Phys. G: Nucl. Part. Phys.* **42**, 034014 (2015).
- [9] B.P. Kay *et al.*, *Phys. Lett. B* **658**, 216 (2008).
- [10] D.K. Sharp *et al.*, *Phys. Rev. C* **87**, 014312 (2013).
- [11] A. Kerek *et al.*, *Phys. Lett. B* **44**, 252 (1973).

- [12] B. Fogelberg, J. Blomqvist, *Nucl. Phys. A* **429**, 205 (1984).
- [13] B. Fogelberg *et al.*, *Phys. Rev. C* **70**, 034312 (2004).
- [14] E.J. Schneid, B. Rosner, *Phys. Rev.* **148**, 1241 (1966).
- [15] P.A. Moore *et al.*, *Phys. Rev.* **175**, 1516 (1968).
- [16] B.P. Kay *et al.*, *Phys. Rev. C* **84**, 024325 (2011).
- [17] B.H. Wildenthal *et al.*, *Phys. Rev. C* **3**, 1199 (1971).
- [18] J.M. Allmond *et al.*, *Phys. Rev. C* **86**, 031307 (2012).
- [19] R.L. Kozub *et al.*, *Phys. Rev. Lett.* **109**, 172501 (2012).
- [20] J.M. Allmond *et al.*, *Phys. Rev. Lett.* **112**, 172701 (2014).
- [21] K.L. Jones *et al.*, *Nature* **465**, 27 (2010).
- [22] L.A. Montestrucque *et al.*, *Nucl. Phys. A* **305**, 29 (1978).
- [23] J.S. Thomas *et al.*, *Phys. Rev. C* **76**, 044302 (2007).
- [24] S. Ahn, "The study of nuclear structure of neutron-rich ^{81}Ge and its contribution in the r-process via the neutron transfer reaction $^{80}\text{Ge}(d, p)$ ", Ph.D. diss., University of Tennessee, 2013, http://trace.tennessee.edu/utk_graddiss/2392
- [25] J.S. Thomas *et al.*, *Phys. Rev. C* **71**, 021302 (2005).
- [26] J.A. Tostevin, University of Surrey, version of the code TWOFNR (of M. Toyama, M. Igarashi and N. Kishida).
- [27] R. Orlandi *et al.*, to be published.
- [28] R. Orlandi *et al.*, *Phys. Lett. B* **740**, 298 (2015).
- [29] D.W. Bardayan *et al.*, *Nucl. Instrum. Methods Phys. Res. A* **711**, 160 (2013).
- [30] V. Bildstein *et al.*, *Eur. Phys. J. A* **48**, 85 (2012).
- [31] N. Warr *et al.*, *Eur. Phys. J. A* **49**, 40 (2013).
- [32] K. Sieja, F. Nowacki, *Phys. Rev. C* **85**, 051301(R) (2012).
- [33] B.P. Kay *et al.*, *J. Phys.: Conf. Ser.* **381**, 012095 (2012).